



Received on 14 March 2025; received in revised form, 30 March 2025; accepted, 15 April 2025; published 01 August 2025

MOLECULAR MAVERICKS: EXPLORING CARBAMATE-HETEROCYCLE CONJUGATES IN THE QUEST FOR EFFECTIVE ALZHEIMER'S THERAPY

Sherin A. Hameed^{*}, N. Fathima, S. Gadha, M. S. Gopika, R. V. Namitha and Sahadiya

Department of Pharmaceutical Chemistry, College of Pharmaceutical Sciences, Govt. Medical College, Thiruvananthapuram - 695011, Kerala, India.

Keywords:

Alzheimer's disease, Cholinesterase inhibitors, Carbamates, Heterocyclic conjugates, Binding affinity, Molecular dynamic simulation

Correspondence to Author:

Dr. Sherin A. Hameed

Assistant Professor,
Department of Pharmaceutical
Chemistry, College of Pharmaceutical
Sciences, Govt. Medical College,
Thiruvananthapuram - 695011,
Kerala, India.

E-mail: sherinirshad@gmail.com

ABSTRACT: Alzheimer's Disease is considered as the most common form of dementia, contributing to about 70% of the cases. The FDA approved Acetyl cholinesterase inhibitors and NMDA receptor antagonists only produce a symptomatic relief and raises the need for novel potential drug candidates for AD management. The various hypotheses on Alzheimer's Disease reveal its multifactorial nature and thus these multiple targets can be considered for the development of new drug molecules. In this study we focus on designing new carbamate-heterocycle molecules with different heterocycles indole, isoquinoline, thiazole, oxazole and 1,2,4- triazines and identifying their multitarget potential through computer aided drug design. The proposed conjugates were docked with the targets Acetyl cholinesterase (AChE), N-methyl-D- Aspartate Receptor (NMDA), and Tyrosinase enzyme. The results indicated that the compound ISO-10 exhibits a high binding affinity for three targets. The target 1FSS demonstrated the highest binding affinity of the three and is suitable for molecular simulation.

INTRODUCTION: Alzheimer's disease (AD), named after German psychiatrist Alois Alzheimer, is a progressive neurodegenerative disease characterized by neuritic plaques and neurofibrillary tangles due to the accumulation of amyloid-beta peptides in the medial temporal lobe and neocortical structures. Alois Alzheimer discovered amyloid plaques and significant neuron loss in his first patient, who suffered from memory loss and personality changes before dying. Emil Kraepelin first named AD in his 8th edition psychiatry handbook. The condition is the most common type of dementia¹.

AD is a progressive neurodegenerative disease and it is defined by loss of cognitive function which includes memory loss, reasoning impairment, and behavioral changes². Of the 6.9 million people aged 65 and older with Alzheimer's dementia in the United States, 4.2 million are women and 2.7 million are men³. The main causes of Alzheimer's disease are thought to be changes in the amyloid β protein and impairment of cholinergic function. Alzheimer's disease is a complex disease that is linked to age, genetics, head injuries, vascular disorders, infections, and environmental factors¹.

Preclinical, mild cognitive impairment (MCI) and dementia are the different stages or phases of Alzheimer's disease. Preclinical patients have no symptoms, but pathology is evident. MCI patients exhibit deficits in memory but function independently. Dementia patients experience severe memory deficits, language alterations, and

<p>QUICK RESPONSE CODE</p> 	<p>DOI: 10.13040/IJPSR.0975-8232.16(8).2275-93</p>
<p>This article can be accessed online on www.ijpsr.com</p>	
<p>DOI link: https://doi.org/10.13040/IJPSR.0975-8232.16(8).2275-93</p>	

difficulty in navigation ⁴. Alzheimer's disease is marked by gradual and progressive neurodegeneration resulting from neuronal cell loss. The neurodegenerative process typically begins in the entorhinal cortex within the hippocampus. Reducing risk may involve higher education, estrogen use, anti-inflammatory agents, and regular exercise ⁴. Computed topography (CT) and magnetic resonance imaging (MRI) were the first imaging modalities employed in AD. Nowadays, PET, fMRI, and SPECT are being increasingly useful for early diagnosis and tracking clinical development ⁵. Cholinesterase inhibitors

Examples: Donepezil, Rivastigmine, Galantamine, Tacrine and partial N-methyl D-aspartate (NMDA) antagonists Example: Memantine are approved as symptomatic therapy for Alzheimer's disease (AD), which is the main strategy used in clinical practice. Aducanemab, Lecanemab, and Donanemab are examples of disease-modifying treatments that use immunotherapy to eliminate amyloid from the brain. The cerebral vascular walls' reaction to amyloid-targeting treatments results in Amyloid Related Imaging Abnormalities (ARIA), which can lead to arterial haemorrhages and capillary leaks ⁶.

Alzheimer's Disease Hypotheses:

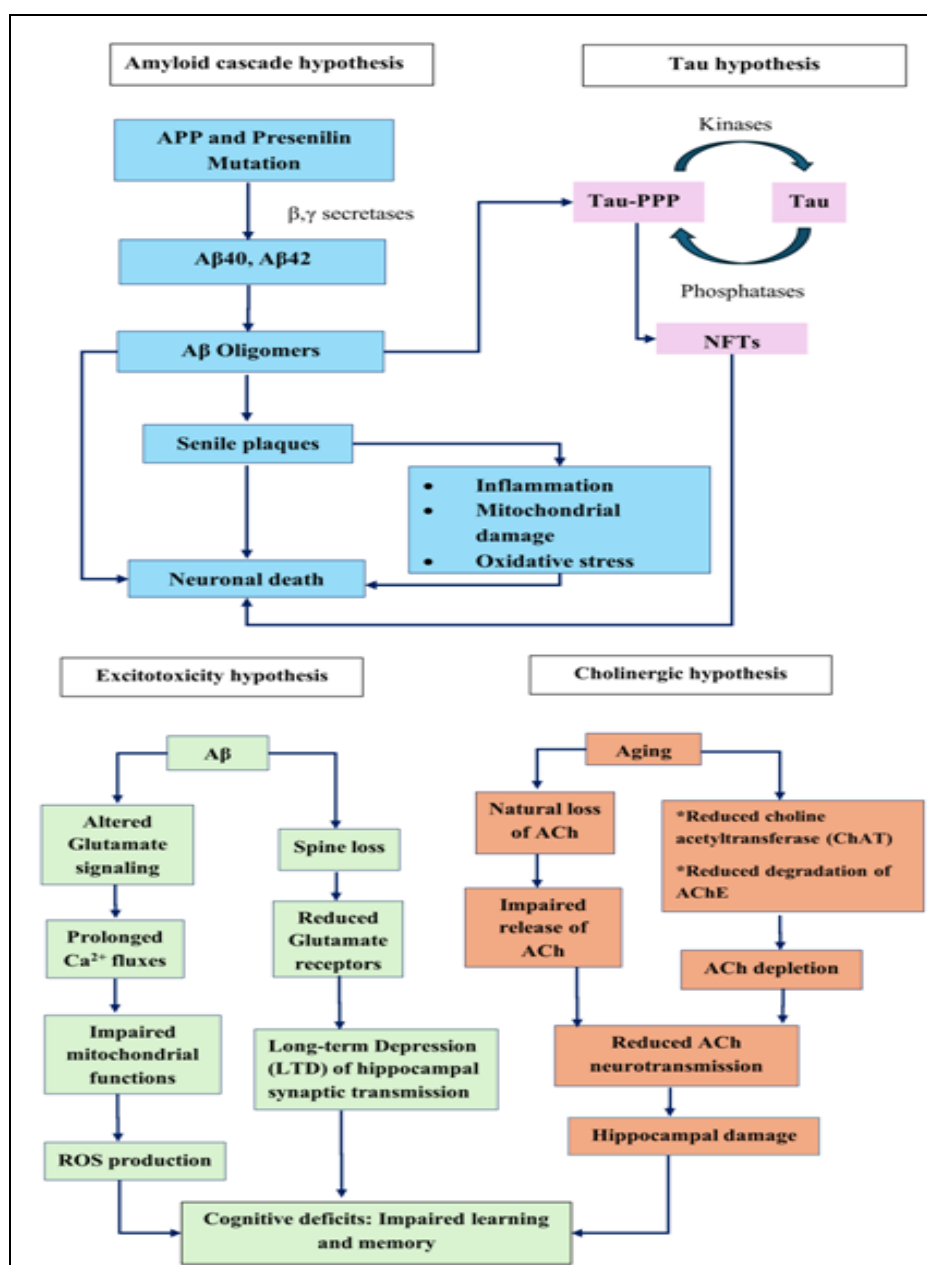


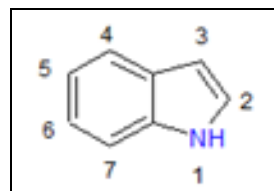
FIG. 1: FLOWCHART OF THE VARIOUS ALZHEIMER'S DISEASE HYPOTHESES ⁷

CARBAMATE- an Important Pharmacophore for Alzheimer's disease Therapy: The biological and pharmacological properties of carbamates are diverse. Interestingly, carbamate-based acetyl cholinesterase (AChE) inhibitors are known to have therapeutic uses in a number of illnesses, including Alzheimer's. A structural motif of many drugs and prodrugs, the carbamate group is a desirable component of the structure of many pharmacologically significant compounds due to its chemical characteristics, conformational and metabolic stability, and the ability to cross cell membranes and, in some cases, the blood-brain barrier⁸. The blood-brain barrier (BBB) can be crossed by substances including rivastigmine, neostigmine, phenserine, and physostigmine, which block cholinesterase activity in the central nervous system (CNS). Therefore, researchers continue to place a great deal of emphasis on creating new carbamate compounds that function as cholinesterase inhibitors⁹.

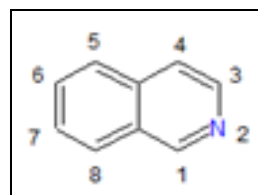
Heterocycles- A Potential Scaffold in Drug Development: The distinctive physical, chemical, and biological characteristics of heterocycles make them a crucial scaffold in medicinal chemistry. Heterocycles are found in around 85% of all chemical entities that are physiologically active. Dipole-dipole interactions, hydrogen bonds, and other biological interactions with the enzymes (receptors) are made possible by the presence of different heteroatoms, such as nitrogen, oxygen, and sulphur, within a ring structure^{10,11}.

INDOLE: The chemical formula for the aromatic heterocyclic ring indole is C_8H_7N . A six-membered benzene ring fused to a five-membered pyrrole ring gives it a bicyclic structure. Indoles are derivatives of indoles in which one or more hydrogen atoms have been swapped out for substituent groups¹². The neurotransmitter serotonin and the amino acid tryptophan are two examples of the many indoles found in nature. One of the main properties of indole molecules is their reactivity with strong acids. This is because the indole ring's aromatic nature makes it easy for it to protonate at the C-3 position,¹³ especially when it comes into contact with strong acids like hydrochloric acid¹⁴. Indole analogues have a wide range of biological activities that make them useful in drug development for a variety of diseases.

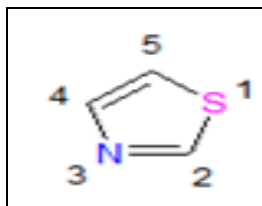
These activities include the potential to be anti-cancer, anti-inflammatory, anti-microbial, anti-viral, anti-hypertensive, anti-diabetic, anti-malarial, and anti-HIV agents^{14,15}.



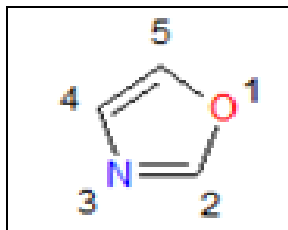
ISOQUINOLINE: Benzopyridines, also known as isoquinolines, are heterocyclic aromatic chemical compounds with formula C_9H_7N that are made up of a pyridine ring fused to a benzene ring. The nitrogen atom is located on the second position of the benzene ring in this structural isomer of quinoline. Although it is more basic than quinoline, it has a weak alkaline character. Because of their potential to express a wide range of biological activities, including anti-malarial, anti-HIV, anti-tumor, anti-fungal, anti-tubercular, anti-glaucoma, anti-bacterial, anti-Parkinson's disease, etc., isoquinoline and its derivatives are found in a variety of natural products and are regarded as pharmacologically active¹⁶.



THIAZOLE: Thiazole is a heterocyclic chemical molecule having the molecular formula C_3H_3NS and a five-membered molecular ring structure. Both an electron-accepting group ($C=N$) and an electron-donating group ($-S-$) are present. According to Huckel's rule, thiazole is aromatic when a single pair of electrons from the Sulphur atom delocalize to complete the desired 6 π electrons. The thiazole ring has become a key synthon to produce a range of NCEs (New Chemical Entities) because of its high reactivity caused by the acidic proton at C-2. Different thiazole ring alterations at various locations produced a range of new compounds with a broad range of pharmacological properties, including diuretics, antioxidants, antibacterial, antifungal, antitubercular, anti-inflammatory, and anticancer properties¹⁷.

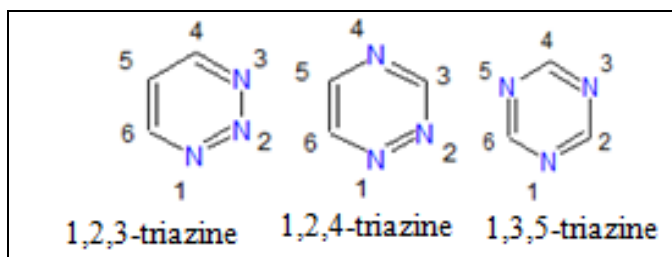


OXAZOLE: Oxazole is a heterocyclic ring structure with five members. The first and third positions are occupied by oxygen and nitrogen respectively. Because of their strong biological activity, oxazole-based molecules have prospective uses in the fields of medicine, chemistry, agriculture, and material sciences. Oxazole derivatives biological actions, such as their antibacterial, anticancer, antitubercular, anti-inflammatory, antidiabetic, anti-obesity, and antioxidant qualities, are greatly influenced by their substitution pattern¹⁸.



TRIAZINE: The triazine structure is a heterocyclic ring, similar to the six-membered benzene with three carbons substituted by nitrogen. The three isomers of triazine are 1,2,3-triazine, 1,2,4-triazine, and 1,3,5-triazines, and are identified by the locations of their nitrogen atoms¹⁹.

The multifunctional nature of 1,2,4-triazine derivatives has drawn a lot of attention, particularly in relation to their varied pharmacological properties. They are also a crucial component of many drug candidates that have demonstrated a variety of pharmacological activities, including anti-diabetic, antifungal, anti-inflammatory, anticancer, anti-HIV, neuroprotective and antioxidant, antiviral, neuroleptic, nootropic, and antiparasitic effects²⁰.



MATERIALS AND METHODS:

Materials:

Protein Targets:

ACETYLCHOLINESTERASE:

Acetylcholinesterase (AChE) is a synaptic enzyme with the principal role of which is believed to be the termination of impulse transmission at the cholinergic synapses by rapid hydrolysis of the neurotransmitter, acetylcholine (ACh).

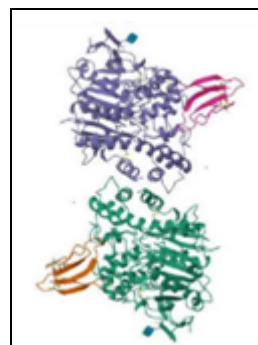


FIG. 2: 3D IMAGE OF THE ENZYME ACETYLCHOLINESTERASE²¹

PDB ID: 1FSS: The three-dimensional (3D) structure of AChE revealed that its active site is located near the bottom of a 20 Å deep and narrow gorge, the surface of which is largely composed of the rings of an array of conserved aromatic amino acids. The active site comprises of two subsites called 'esteratic' and 'anionic or aromatic' subsites. The esteratic subsite contains a catalytic triad of three amino acids, Serine 203, Histidine 447 and Glutamate 324. Residues Tryptophan 86 and Tyrosine 337 constitute the 'anionic or aromatic' subsite of the catalytic site (CAS), making π -cation interactions with the quaternary group of the substrate. The Tyrosine 337, termed as a 'swinging gate', has a critical role in the binding of substrates and various inhibitors. Residues Tryptophan 286 and Tyrosine 72 contribute to the peripheral anionic site or peripheral aromatic site (PAS), located at the lip of the gorge has an important role in routing the substrate perfectly to the active site. The Phenylalanine at 295 and 297 contributes to the acyl pocket, which determines the specificity for ACh²².

N-Methyl-D-Aspartate (NMDA): N-methyl-d-aspartate receptor (NMDAR)-mediated excitatory signalling is essential for neurological illnesses and disorders as well as brain growth and function. Because NMDAR channel blockers may be used to

treat epilepsy, depression, and Alzheimer's disease, they are of medical importance²³. N-methyl-D-aspartate (NMDA) receptors are ligand-gated ion channels that are activated by excitatory neurotransmitters. These N-methyl-D-aspartate receptors (NMDAR) are involved in excitatory neurotransmission in the central nervous system because they are mostly located at excitatory synapses²⁴.

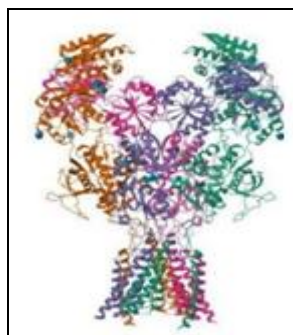


FIG. 3: 3D IMAGE OF THE RECEPTOR N-METHYL-D-ASPARTATE²⁵

PDB ID: 7SAD: N-methyl-D-aspartate receptors (NMDARs) are ion channels in the central nervous system that react to the neurotransmitter glutamate. They play a crucial role in synaptic transmission, learning, memory, plasticity, and excitotoxicity. The majority of NMDARs consist of two mandatory GluN1 subunits and regulatory subunits GluN2 and GluN3²⁶. They are abundantly dispersed throughout the CNS and are involved in cognitive processes and neurodegenerative diseases like Parkinson's and Alzheimer's²⁷. The GluN2 subunit has distinct expression patterns during development and different regions. GluN2A progressively increases after birth in the brain until adulthood, while GluN2B peaks around postnatal day seven. This phenomenon is known as the developmental GluN2B-GluN2A switch, where GluN2A expression rises while GluN2B remains constant²⁸.

TYROSINASE: Tyrosinases belong to the class of oxidases present in both plant and animal tissues that catalyze melanogenesis, by first hydroxylating L-tyrosine to 3,4-Dihydroxy L phenylalanine (L-DOPA) and then oxidizing L-DOPA to make dopaquinone. All tyrosinases have in common a binuclear, type 3 copper centre within their active sites. The two copper ions in the conserved active site, CuA and CuB, are coordinated by six histidine residues^{26, 29}.

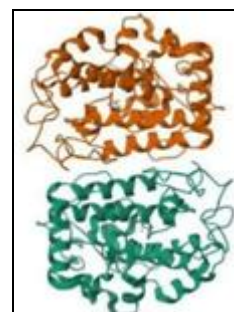


FIG. 4: 3D IMAGE OF THE ENZYME TYROSINASE³⁰

PDB ID: 5I38: The overall structure of tyrosinase can be divided into three domains: the central domain, the N-terminal domain, and the C-terminal domain. The central domain, which is composed of six conserved histidine residues, contains the CuA and CuB oxidizing ions. Although, it is the most conserved domain among tyrosinases, CO and Hc, the CuB site exhibits higher conservation than CuA. Biochemical investigations of tyrosinases from distinct species have shown the involvement of the conserved histidine residues in copper binding²⁹.

Methods:

Design of Proposed Ligands: ACD/Chemsketch Software is used for drawing the structures of the proposed carbamate- heterocycles and to determine chemical properties of the molecules for our study. After drawing the molecule, it is selected, and clean-up is conducted. The designed molecules are saved in sdf format.

In-silico Drug Design: *In-silico* design of the proposed ligands are conducted using PASS online, Molinspiration, SwissADME, Swiss Target Prediction, ProTox 3.0.

- PASS online is used to predict the activity spectra of the designed molecules, this is conducted by pasting the canonical smiles generated using ACD/Chem sketch Software.
- Molinspiration Software is used to find whether the designed molecules obeyed the Lipinski's Rule of Five and Drug Likeness (Bioactivity score).
- SwissADME, Swiss Target Prediction is used to calculate physiochemical and pharmacokinetic properties, Boiled egg model to predict gastrointestinal or Blood Brain Barrier permeation, Bioavailability Radar to

determine whether the proposed ligands are orally bioavailable.

- ProTox 3.0 webserver to predict the toxicity, toxicity endpoints, organ toxicity of the proposed ligands.

Molecular Docking:

- Target structure selection: Download the protein from RCSB PDB in PDB format and open the structure in Biovia Discovery Studio, then prepare the protein.
- Ligand selection: Download the standard ligand from PubChem in SDF format and ChemSketch Software is used for drawing the structures of the proposed carbamate - heterocycles.
- Docking is a computer simulation technique used to predict the preferred orientation of two interacting chemical species. The molecular interaction analysis of the targets and ligand molecules are performed using PyRx-0.8 software.
- Receptor ligand interactions are analyzed by using Biovia Discovery Studio.

Molecular Dynamic Simulation: The molecular interaction analysis of the target (PDB: 1FSS) and ligand molecule (ISO-10) is performed using

Autodock vina software (v.1.2.0.). The MD simulations were performed using GROMACS version 2022.1 MD package running on Ubuntu 22.04.1 (AMD® Ryzen 9 3900 x 12- core processor x 24).

The process was initiated by removing crystal water from the structures, followed by generating topology files. For the docked complex, the topology file for protein was generated using the Charmm36 force field (Charmm 36 jul 2021.ff)

RESULTS AND DISCUSSION:

Design of Proposed Ligands and Lipinski's Rule Analysis: In this study, the different carbamates which are conjugated with Indole, Isoquinoline, Thiazole, Oxazole and 1,2,4- triazine were designed using ACD/Chemsketch FREEWARE and the smiles notation of the 80 newly designed conjugates were found out for further *in-silico* studies. General Structure of carbamate- indole conjugates.

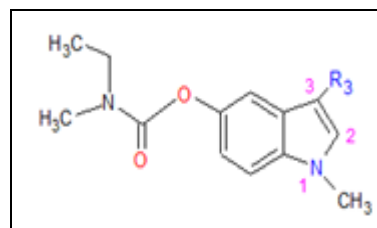
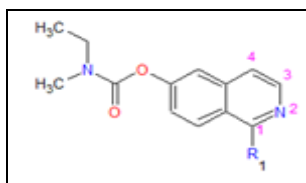


TABLE 1: SMILES NOTATION AND LIPINSKI'S RULE ANALYSIS OF CARBAMATE- INDOLE CONJUGATES

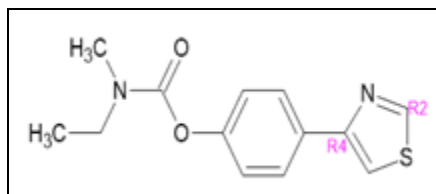
Ligand code	R ₃ substituent	SMILES notation	Log P	MW	HA C	HD O	Rot b
IND-1	-CH ₃	CCN(C)C(=O)Oc1ccc2c(c1)c(C)cn2C	2.58	246.31	4	0	3
IND-2	-NH ₂	CCN(C)C(=O)Oc1ccc2c(c1)c(N)cn2C	1.61	247.30	5	2	3
IND-3	-OH	CCN(C)C(=O)Oc1ccc2c(c1)c(O)cn2C	1.91	248.28	5	1	3
IND-4	-CH ₂ OH	CCN(C)C(=O)Oc1ccc2c(c1)c(CO)cn2C	1.47	262.31	5	1	4
IND-5	-Cl	CCN(C)C(=O)Oc1ccc2c(c1)c(Cl)cn2C	2.81	266.73	4	0	3
IND-6	-Br	CCN(C)C(=O)Oc1ccc2c(c1)c(Br)cn2C	2.94	311.18	4	0	3
IND-7	-COOH	CCN(C)C(=O)Oc1ccc2c(c1)c(C(=O)O)cn2C	1.70	276.29	6	1	4
IND-8	-CONH ₂	CCN(C)C(=O)Oc1ccc2c(c1)c(C(N)=O)cn2C	0.95	275.31	6	2	4
IND-9	-CN	CCN(C)C(=O)Oc1ccc2c(c1)c(C#N)cn2C	1.10	257.29	5	0	3
IND-10	-CF ₃	CCN(C)C(=O)Oc1ccc2c(c1)c(C(F)(F)F)cn2C	3.03	300.28	4	0	4
IND-11	-OCH ₃	CCN(C)C(=O)Oc1ccc2c(c1)c(OC)cn2C	2.19	262.31	5	0	4
IND-12	-SO ₃ H	CCN(C)C(=O)Oc1ccc2c(c1)c(S(=O)(=O)O)cn2C	-0.88	312.35	7	1	4
IND-13	-COCH ₃	CCN(C)C(=O)Oc1ccc2c(c1)c(C(C)=O)cn2C	2.03	274.32	5	0	4
IND-14	-NO ₂	CCN(C)C(=O)Oc1ccc2c(c1)c(N(=O)=O)cn2C	2.09	277.28	7	0	4
IND-15	=O	CCN(C)C(=O)Oc1ccc2c(c1)C(=O)CN2C	1.35	248.78	5	0	3
IND-16	-NHCOCH ₃	CCN(C)C(=O)Oc1ccc2c(c1)c(NC(C)=O)cn2C	1.35	289.33	6	1	4

General structure of carbamate- isoquinoline conjugates

**TABLE 2: SMILES NOTATION AND LIPINSKI'S RULE ANALYSIS OF CARBAMATE- ISOQUINOLINE CONJUGATES**

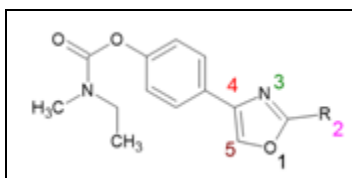
Ligand code	R ₁ substituent	Smiles notation	Log P	MW	HAC	HDO	Rot b
ISO-1	-CH ₃	CN(CC)C(=O)Oc1cc2ccnc(C)c2cc1	2.25	244.29	4	0	3
ISO-2	-NH ₂	CN(CC)C(=O)Oc1cc2ccnc(N)c2cc1	1.63	245.28	5	2	3
ISO-3	-OH	CN(CC)C(=O)Oc1cc2ccnc(O)c2cc1	1.93	246.27	5	1	4
ISO-4	-CH ₂ OH	CN(CC)C(=O)Oc1cc2ccnc(CO)c2cc1	1.60	260.29	5	1	4
ISO-5	-Cl	CN(CC)C(=O)Oc1cc2ccnc(Cl)c2cc1	2.83	264.71	4	0	3
ISO-6	-Br	CN(CC)C(=O)Oc1cc2ccnc(Br)c2cc1	2.96	309.16	4	0	3
ISO-7	-COOH	CN(CC)C(=O)Oc1cc2ccnc(C(=O)O)c2cc1	1.84	274.28	6	1	4
ISO-8	-CONH ₂	CN(CC)C(=O)Oc1cc2ccnc(C(=O)N)c2cc1	1.08	273.29	6	2	4
ISO-9	-CN	CN(CC)C(=O)Oc1cc2ccnc(C#N)c2cc1	2.02	255.28	5	0	3
ISO-10	-CF ₃	O=C(Oc1cc2ccnc(c2cc1)C(F)(F)F)N(C)CC	3.16	298.26	4	0	4
ISO-11	-OCH ₃	COc1cccc2cc(c1cc2)OC(=O)N(C)CC	2.21	260.29	5	0	4
ISO-12	-SO ₃ H	CN(CC)C(=O)Oc1cc2C=CNC(c2cc1)S(=O)(=O)O	0.69	310.33	7	1	4
ISO-13	-COCH ₃	CN(CC)C(=O)Oc1cc2ccnc(c2cc1)C(C)=O	2.16	272.30	5	0	4
ISO-14	-NO ₂	CN(CC)C(=O)Oc1cc2ccnc([N+](=O)[O-])c2cc1	2.11	275.26	7	0	4
ISO-15	=O	CN(CC)C(=O)Oc1cc2C=CNC(=O)c2cc1	1.47	246.27	5	0	3
ISO-16	-NHCOCH ₃	CN(CC)C(=O)Oc1cc2ccnc(NC(C)=O)c2cc1	1.37	287.32	6	1	4

General Structure of carbamate- thiazole conjugates

**TABLE 3: SMILES NOTATION AND LIPINSKI'S RULE ANALYSIS OF CARBAMATE- THIAZOLE CONJUGATES**

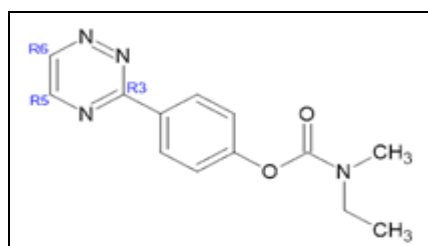
Ligand code	R ₂ substituent	SMILES notation	Log P	MW	HAC	HDO	Rot b
THIA-1	-CH ₃	CCN(C)C(=O)Oc2ccc(c1csc(C)n1)cc2	2.25	276.36	4	0	4
THIA-2	-NH ₂	CCN(C)C(=O)Oc2ccc(c1csc(N)n1)cc2	2.15	277.35	5	2	4
THIA-3	-OH	CCN(C)C(=O)Oc2ccc(c1csc(O)n1)cc2	2.44	278.33	5	1	4
THIA-4	-CH ₂ OH	CCN(C)C(=O)Oc2ccc(c1csc(CO)n1)cc2	1.61	292.36	5	1	5
THIA-5	-Cl	CCN(C)C(=O)Oc2ccc(c1csc(Cl)n1)cc2	3.34	296.78	4	0	4
THIA-6	-Br	CCN(C)C(=O)Oc2ccc(c1csc(Br)n1)cc2	3.47	341.21	4	0	4
THIA-7	-COOH	CCN(C)C(=O)Oc2ccc(c1csc(C(=O)O)n1)cc2	1.84	306.34	6	1	5
THIA-8	-CONH ₂	CCN(C)C(=O)Oc2ccc(c1csc(C(N)=O)n1)cc2	1.09	305.36	6	2	5
THIA-9	-CN	CCN(C)C(=O)Oc2ccc(c1csc(C#N)n1)cc2	2.03	287.34	5	0	4
THIA-10	-CF ₃	CCN(C)C(=O)Oc2ccc(c1csc(C(F)F)n1)cc2	3.17	330.33	4	0	5
THIA-11	-OCH ₃	CCN(C)C(=O)Oc2ccc(c1csc(OC)n1)cc2	2.72	292.36	5	0	5
THIA-12	-SO ₃ H	CCN(C)C(=O)Oc2ccc(c1csc(S(=O)(=O)O)n1)cc2	0.18	342.40	7	1	5
THIA-13	-COCH ₃	CCN(C)C(=O)Oc2ccc(c1csc(C(C)=O)n1)cc2	2.17	304.37	5	0	5
THIA-14	-NO ₂	CCN(C)C(=O)Oc2ccc(c1csc(N(=O)=O)n1)cc2	2.62	307.33	7	0	5
THIA-15	=O	CCN(C)C(=O)Oc2ccc(c1csc(=O)[nH]1)cc2	1.99	278.33	5	1	4
THIA-16	-NHCOCH ₃	CCN(C)C(=O)Oc2ccc(c1csc(NC(C)=O)n1)cc2	1.88	321.40	6	2	5

General Structure of carbamate- oxazole conjugates

**TABLE 4: SMILES NOTATION AND LIPINSKI'S RULE ANALYSIS OF CARBAMATE- OXAZOLE CONJUGATES**

Ligand code	R ₂ substituent	SMILES notation	Log P	MW	HAC	HDO	Rot b
OXA-1	-CH ₃	CCN(C)C(=O)Oc2ccc(c1coc(C)n1)cc2	2.12	260.29	5	0	4
OXA-2	-NH ₂	CCN(C)C(=O)Oc2ccc(c1coc(N)n1)cc2	1.51	261.28	6	2	4
OXA-3	-OH	CCN(C)C(=O)Oc2ccc(c1coc(O)n1)cc2	1.80	262.26	6	1	4
OXA-4	-CH ₂ OH	CCN(C)C(=O)Oc2ccc(c1coc(CO)n1)cc2	1.48	276.29	6	1	5
OXA-5	-Cl	CCN(C)C(=O)Oc2ccc(c1coc(Cl)n1)cc2	2.70	280.71	5	0	4
OXA-6	-Br	CCN(C)C(=O)Oc2ccc(c1coc(Br)n1)cc2	2.83	325.16	5	0	4
OXA-7	-COOH	CCN(C)C(=O)Oc2ccc(c1coc(C(=O)O)n1)cc2	1.71	290.27	7	1	5
OXA-8	-CONH ₂	CCN(C)C(=O)Oc2ccc(c1coc(C(N)=O)n1)cc2	0.96	289.29	7	2	5
OXA-9	-CN	CCN(C)C(=O)Oc2ccc(c1coc(C#N)n1)cc2	1.89	271.28	6	0	4
OXA-10	-CF ₃	CCN(C)C(=O)Oc2ccc(c1coc(C(F)(F)F)n1)cc2	3.03	314.26	5	0	5
OXA-11	-OCH ₃	CCN(C)C(=O)Oc2ccc(c1coc(OC)n1)cc2	2.08	276.29	6	0	5
OXA-12	-SO ₃ H	CCN(C)C(=O)Oc2ccc(c1coc(S(=O)(=O)O)n1)cc2	-0.82	326.33	8	1	5
OXA-13	-COCH ₃	CCN(C)C(=O)Oc2ccc(c1coc(C(C)=O)n1)cc2	2.04	288.30	6	0	5
OXA-14	-NO ₂	CCN(C)C(=O)Oc2ccc(c1coc(N(=O)=O)n1)cc2	1.98	291.26	8	0	5
OXA-15	=O	CCN(C)C(=O)Oc2ccc(c1coc(=O)[nH]1)cc2	1.35	262.26	6	1	4
OXA-16	-NHCOCH ₃	CCN(C)C(=O)Oc2ccc(c1coc(NC(C)=O)n1)cc2	1.24	303.32	7	1	5

General Structure of carbamate-1,2,4- triazine conjugates

**TABLE 5: SMILES NOTATION AND LIPINSKI'S RULE ANALYSIS OF CARBAMATE- 1,2,4-TRIAZINE CONJUGATES**

Ligand code	R ₆ substituent	SMILES notation	Log P	MW	HAC	HDO	Rot b
TRI-1	-CH ₃	CCN(C)C(=O)Oc2ccc(c1ncc(C)nn1)cc2	2.03	272.31	6	0	4
TRI-2	-NH ₂	CCN(C)C(=O)Oc2ccc(c1ncc(N)nn1)cc2	1.42	273.30	7	2	4
TRI-3	-OH	CCN(C)C(=O)Oc2ccc(c1ncc(O)nn1)cc2	1.72	274.28	7	1	4
TRI-4	-CH ₂ OH	CCN(C)C(=O)Oc2ccc(c1ncc(CO)nn1)cc2	1.39	288.31	7	1	5
TRI-5	-Cl	CCN(C)C(=O)Oc2ccc(c1ncc(Cl)nn1)cc2	2.61	292.73	6	0	4
TRI-6	-Br	CCN(C)C(=O)Oc2ccc(c1ncc(Br)nn1)cc2	2.75	337.18	6	0	4
TRI-7	-COOH	CCN(C)C(=O)Oc2ccc(c1ncc(C(=O)O)nn1)cc2	1.62	302.29	8	1	5
TRI-8	-CONH ₂	CCN(C)C(=O)Oc2ccc(c1ncc(C(N)=O)nn1)cc2	0.87	301.31	8	2	5
TRI-9	-CN	CCN(C)C(=O)Oc2ccc(c1ncc(C#N)nn1)cc2	1.81	283.29	7	0	4
TRI-10	-CF ₃	CCN(C)C(=O)Oc2ccc(c1ncc(C(F)(F)F)nn1)cc2	2.95	326.28	6	0	4
TRI-11	-OCH ₃	CCN(C)C(=O)Oc2ccc(c1ncc(OC)nn1)cc2	1.99	288.31	7	0	5
TRI-12	-SO ₃ H	CCN(C)C(=O)Oc2ccc(c1ncc(S(=O)(=O)O)nn1)cc2	-0.91	338.35	9	1	5
TRI-13	-COCH ₃	CCN(C)C(=O)Oc2ccc(c1ncc(C(C)=O)nn1)cc2	1.95	300.32	7	0	5
TRI-14	-NO ₂	CCN(C)C(=O)Oc2ccc(c1ncc(N(=O)=O)nn1)cc2	1.90	303.28	9	0	5
TRI-15	=O	CCN(C)C(=O)Oc2ccc(c1ncc(=O)[nH]1)cc2	1.26	274.28	7	1	4
TRI-16	-NHCOCH ₃	CCN(C)C(=O)Oc2ccc(c1ncc(NC(C)=O)nn1)cc2	1.15	315.33	8	1	5

Lipinski's Rule of Five Analysis: Lipinski's rule of five is a rule of thumb to evaluate drug likeness, or to determine if a chemical compound with a certain pharmacological activity has properties that

would make it a likely orally active drug in humans. Compounds violating more than one of these rules may have problems with their bioavailability. These descriptors are calculated by using Molinspiration software.

In general, an orally active drug has:

- ✓ Not more than 5 hydrogen bond donors
- ✓ Not more than 10 hydrogen bond acceptors
- ✓ Molecular weight not higher than 500
- ✓ Calculated octanol/water partition (log P) not higher than 5
- ✓ The number of rotatable bonds in a given molecule should be kept below 10³¹.

All the proposed ligands followed Lipinski's Rule of Five with no violations.

Drug Likeness Analysis: In drug design, drug likeness is a qualitative notion used to describe the relative "drug like" nature of a material, estimated by using Molinspiration software. Drug likeness may be defined as a complex balance of various molecular properties and the structural features, which determine whether a particular compound is similar to the known drugs. These properties mainly hydrophobicity, electronic distribution, hydrogen bonding characteristics, molecular weight, flexibility and the presence of various pharmacophoric features influence the behaviour of the molecules in a living organism, including bioavailability, transport properties, affinity to proteins, reactivity, toxicity, metabolic stability and many others.

The Drug likeness analysis of the standard drugs and the proposed conjugates were conducted. The standard drugs Rivastigmine and Donepezil are acetyl cholinesterase inhibitors, their enzyme inhibitor bioactivity scores were compared to that of the proposed ligands under study. The proposed ligands were found to be moderately active.

PASS Prediction: PASS (Prediction of Activity Spectra for Substances)^{32, 33} is a software designed as a tool for evaluating the general biological potential of an organic like molecule. PASS provides simultaneous predictions of many types of

biological activity based on the structure of organic compounds. The Biological activity spectra of the compounds were analyzed. The following activities such as cholinergic activity, Nootropic activity, neurodegenerative diseases treatment, Alzheimer's disease treatment, of the compounds were predicted. But NMDA Receptor Antagonist activity was not predicted in any of the proposed ligands.

Pharmacokinetic Evaluation: In addition to predicting ADME parameters, pharmacokinetic features, drug nature, and medicinal chemistry friendliness of one or more small compounds, SwissADME software^{34, 35} is a web server that facilitates drug discovery. The fate of a therapeutic chemical in the body is explained by its pharmacokinetics. These ADME (Absorption, Distribution, Metabolism, and Excretion) factors can then be assessed independently using specific techniques. In order to anticipate ADME, computer models have been promoted as a viable substitute for experimental methods.

Boiled- Egg Model Analysis: During the various stages of the drug discovery process, intestinal absorption and brain penetration are the two important pharmacokinetic behaviours that must be estimated. This accurate prediction model determines a small compound's lipophilicity and polarity. Every area in the egg model that is colored yellow, white, and grey. A yellow area indicates the greatest chance of entering the brain, a white area indicates the maximum absorption in the GI tract, and a grey area indicates the least chance of entering the brain³⁶.

Graphical output (boiled egg) of the proposed carbamate – indole conjugates.

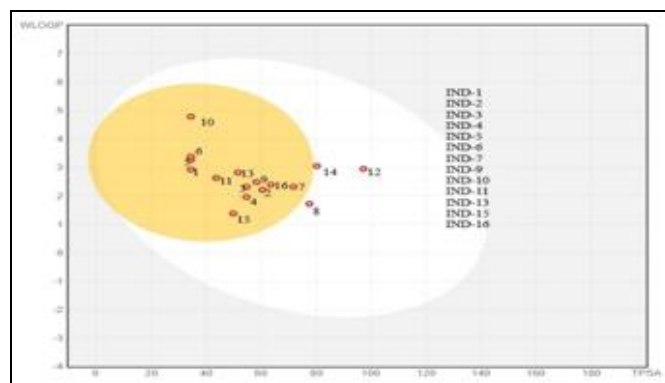


FIG. 5: BOILED EGG DIAGRAM OF PROPOSED CARBAMATE-INDOLE CONJUGATES

The compounds IND-1, IND-2, IND-3, IND-4, IND-5, IND-6, IND-7, IND-9, IND-10, IND-11, IND-13, IND-15, IND-16 lies inside the yolk region, thus showed BBB permeation, while IND-8, IND-12, IND-14 lies in the white portion are likely to be absorbed by the GIT. The results are depicted in the above **Fig. 5**.

Graphical output (boiled egg) of the proposed carbamate – isoquinoline conjugates.

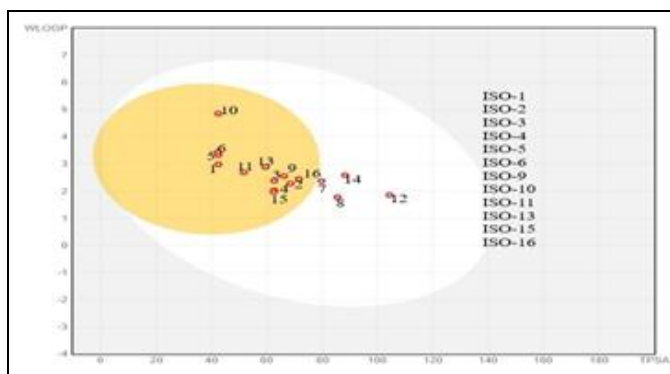


FIG. 6: BOILED EGG DIAGRAM OF PROPOSED CARBAMATE-ISOQUINOLINE CONJUGATES

The compounds ISO-1, ISO-2, ISO-3, ISO-4, ISO-5, ISO-6, ISO-9, ISO-10, ISO-11, ISO-13, ISO-15, ISO-16 lies in the egg yolk (yellow region), thus it shows BBB penetration, whereas ISO-7, ISO-8, ISO-12, ISO-14 in the white portion is likely to be absorbed by the gastrointestinal region. The results are depicted in the above **Fig. 6**.

Graphical output (Boiled egg) of the proposed carbamate -thiazole conjugates.

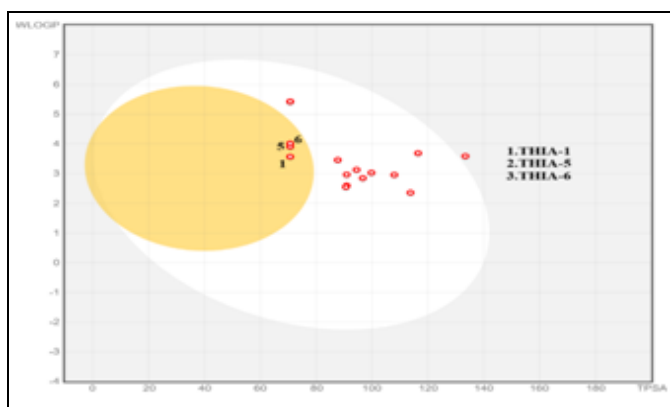


FIG. 7: BOILED EGG DIAGRAM OF PROPOSED CARBAMATE-THIAZOLE CONJUGATES

The compounds THIA-1, THIA-5, THIA-6 lie in the egg yolk (yellow region), thus it shows BBB penetration whereas all the other compounds in the white portion are likely to be absorbed by the

gastrointestinal region. The results are depicted in the above **Fig. 7**.

Graphical output (Boiled egg) of the proposed carbamate- oxazole conjugates.

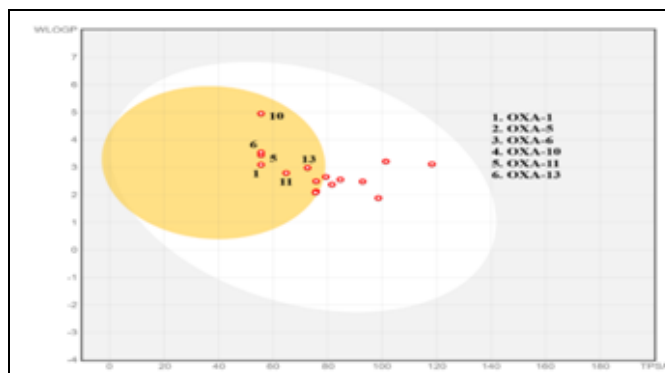


FIG. 8: BOILED EGG DIAGRAM OF PROPOSED CARBAMATE-OXAZOLE CONJUGATES

The compounds OXA-1, OXA-5, OXA-6, OXA-10, OXA-11, OXA-13 lie in the egg yolk (yellow region), thus it shows BBB penetration whereas all the other compounds in the white portion are likely to be absorbed by the gastrointestinal region. The results are depicted in the above **Fig. 8**.

Graphical output (Boiled egg) of the proposed carbamate –1,2,4-triazine conjugates.

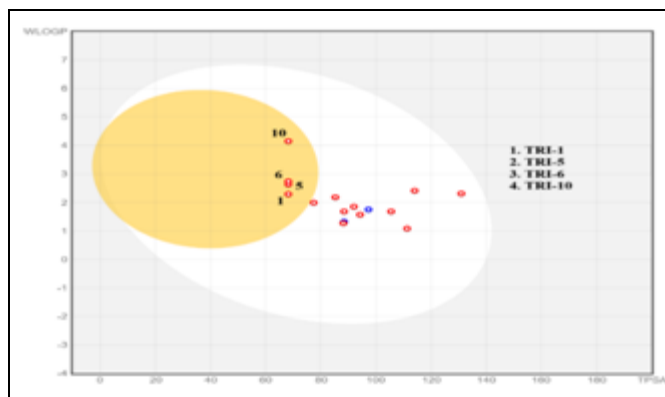


FIG. 9: BOILED EGG DIAGRAM OF PROPOSED CARBAMATE-1,2,4-TRIAZINE CONJUGATES

The Compounds TRI-1, TRI-5, TRI-6, TRI-10 showed BBB permeation (lies in the yellow region), whereas all the other compounds in the white portion are likely to be absorbed by the gastrointestinal region. The results are depicted in the above **Fig. 9**.

Bioavailability Radar Analysis: An effective method for figuring out if a chemical molecule is orally bioavailable is the SwissADME

bioavailability radar analysis. Numerous physicochemical characteristics, such as size, polarity, solubility, flexibility, saturation, and lipophilicity, affect ^{37, 38} it. Using bioavailability

radar, the suggested compounds that were located in the yellow area of the cooked egg model were examined for oral bioavailability.

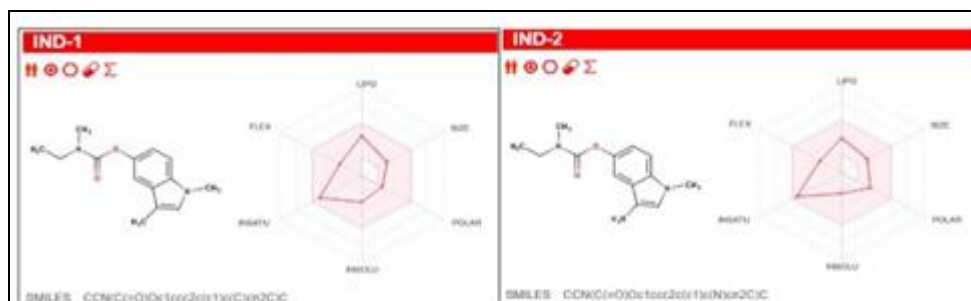


FIG. 10: BIOAVAILABILITY RADAR OF IND-1, IND-2

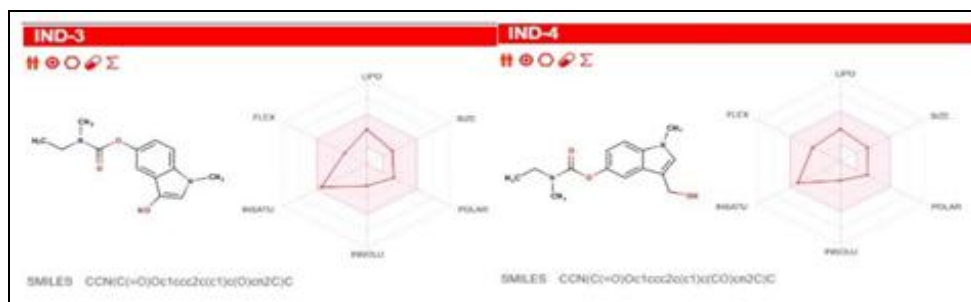


FIG. 11: BIOAVAILABILITY RADAR OF IND-3, IND-4

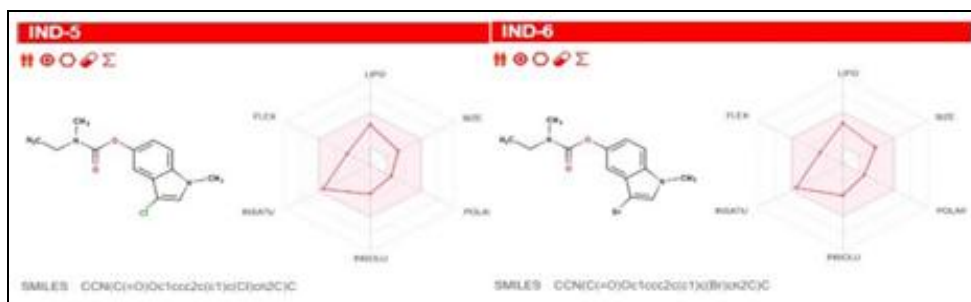


FIG. 12: BIOAVAILABILITY RADAR OF IND-5, IND-6

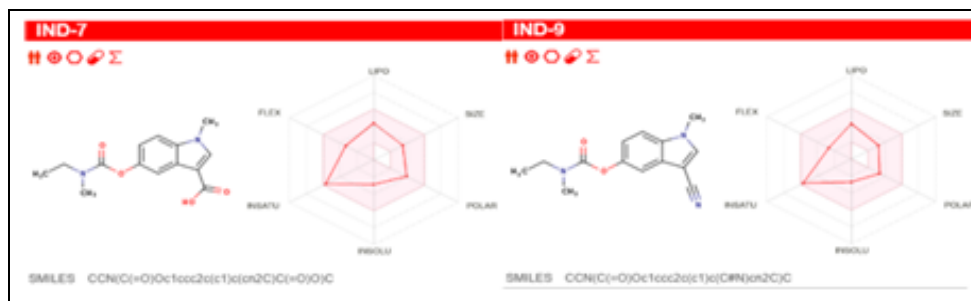


FIG. 13: BIOAVAILABILITY RADAR OF IND-7, IND-9

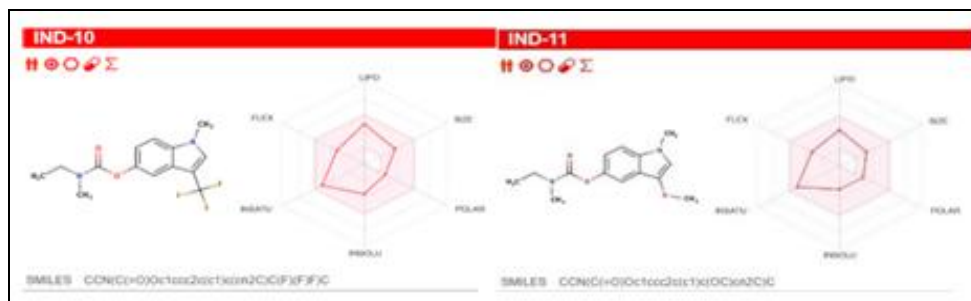


FIG. 14: BIOAVAILABILITY RADAR OF IND-10, IND-11



FIG.15: BIOAVAILABILITY RADAR OF IND-13, IND-15

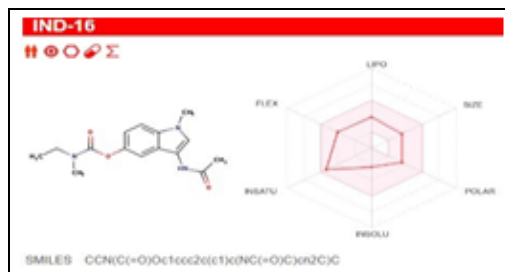


FIG. 16: BIOAVAILABILITY RADAR OF IND-16

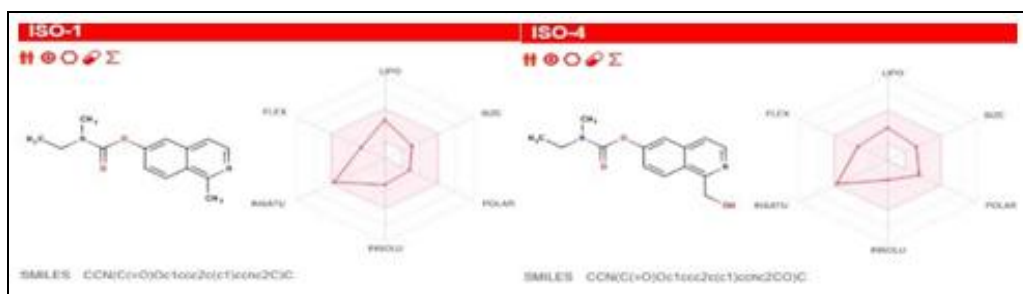


FIG. 17: BIOAVAILABILITY RADAR OF ISO-1, ISO-4



FIG. 18: BIOAVAILABILITY RADAR OF ISO-10, ISO-11



FIG. 19: BIOAVAILABILITY RADAR OF ISO-13, ISO-16



FIG. 20: BIOAVAILABILITY RADAR OF THIA-1

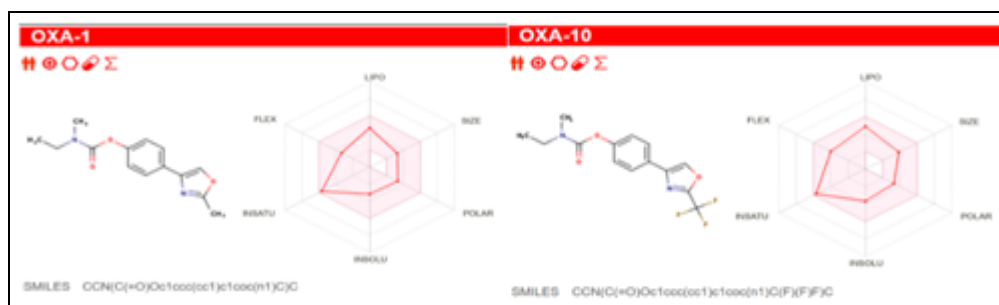
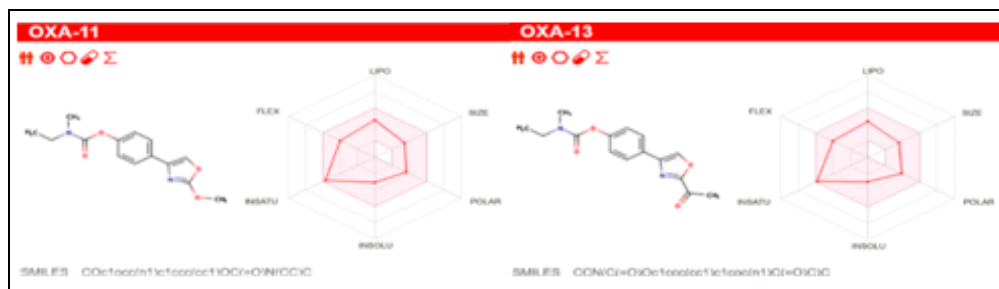
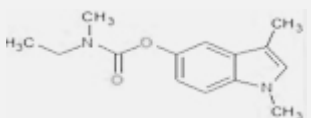
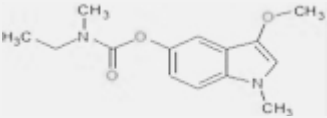
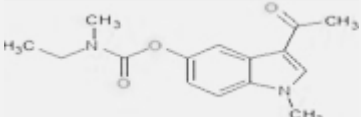
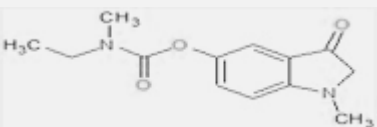
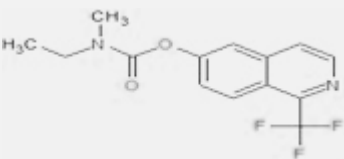
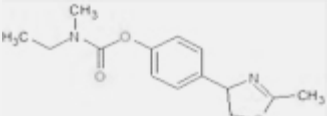
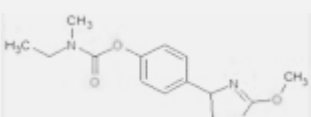
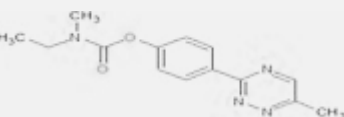


FIG. 21: BIOAVAILABILITY RADAR OF OXA-1, OXA-10

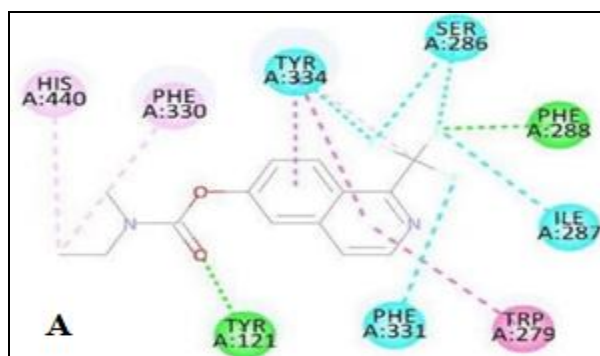


On analysing the results, it was found that ISO-10 has greater binding affinity towards both the targets.

TABLE 7: STRUCTURE & BINDING AFFINITIES OF THE CARBAMATE- HETEROCYCLE CONJUGATES

Compound	Structure	Docking Score		
		PDB ID: 1FSS	PDB ID: 7SAD	PDB ID: 5I38
IND-1		-7.2	-5.7	-6.3
IND-11		-7.1	-6.1	-6.5
IND-13		-7.2	-6.3	-6.3
IND-15		-7.2	-5.7	-6.4
ISO-10		-9.6	-7.1	-7.1
THIA-1		-7.0	-6.8	-7.1
OXA-11		-6.8	-6.5	-7.1
TRI-1		-7.5	-6.7	-7.4

From the docking score analysis, ISO-10 was found to have the highest binding affinity of -9.6, -7.1, -7.1 with PDB; 1FSS, 7SAD, 5I38 respectively.



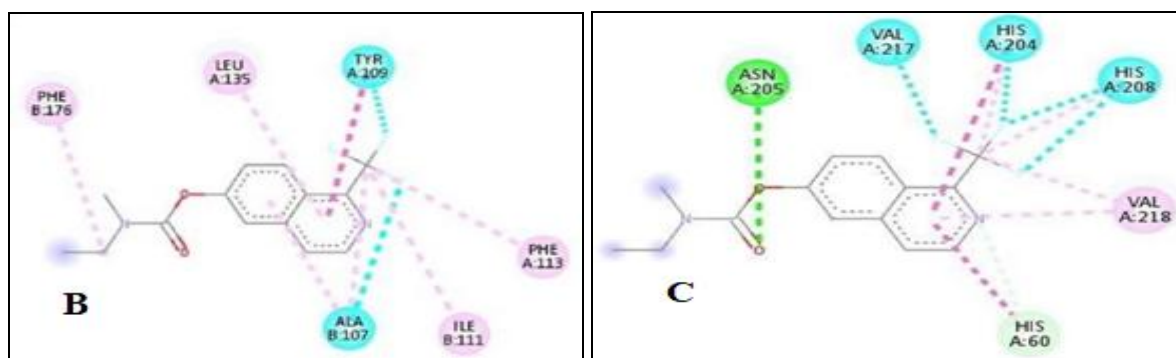
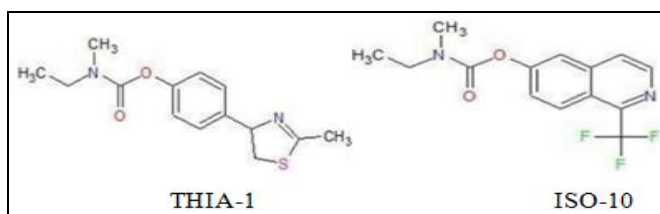


FIG. 24: LIGAND INTERACTION DIAGRAMS A) 'ISO-10 1FSS' DOCKED COMPLEX B) ISO-10 7SAD DOCKED COMPLEX C) ISO-10 5I38 DOCKED COMPLEX

SAR Developed using Docking Score Analysis:

From the docking score analysis **Table 7**, it is observed that the strategic replacement of the phenyl ring (Eg: THIA-1), with a fused ring such as

isoquinoline (Eg: ISO-10) enhanced its inhibitory activity against Acetylcholinesterase, NMDA receptor, and Tyrosinase Enzyme.



Among the other compounds with phenyl substituted rings, 1,2,4-triazine containing compound showed high docking score compared to others with 1,3- thiazole and 1,3- oxazole rings. Electron withdrawing group $-CF_3$, as in the compound ISO-10 showed the best binding affinity compared with other substituents.

Molecular Simulation Results: From the docking results, the compound ISO-10, with the highest binding affinity, was subjected to Molecular Dynamic Simulation. The compound was again docked using Autodock vina software (v.1.2.0.). The ligand "ISO - 10" demonstrated the strongest binding affinity (-8.2 kcal/mol) but did not exhibit any hydrogen bond interactions. Multiple ligands showed similar binding affinities (-8.2, -8.1, and -

8.0 kcal/mol), with the ligand having a binding affinity of -8.1 kcal/mol forming a single hydrogen bond with SER 122. Ligands interacting with TYR 121 consistently formed a single hydrogen bond, with binding affinities ranging from -7.8 to -7.4 kcal/mol. Notably, the ligand (Pose 5) with a binding affinity of -8.0 kcal/mol formed two hydrogen bonds with PHE 288 and TYR 121, making it a particularly promising candidate for further investigation.

Interaction analysis of the receptor-ligand complex was performed using Discovery Studio Biovia 2017. Poses with the best binding affinity and H-bond interaction were selected and subjected to Molecular Dynamic Simulation to validate the interaction stability.

TABLE 8: ISO-10 1FSS DOCKED RESULT

Sl. no.	Ligand	Affinity (kcal/mol)	H-bond Interactions	No: of H- bond Interactions
1.	ISO-10	-8.2	SER 122 PHE 288, TYR 121 TYR 121 TYR 121 TYR 121 TYR 121 TYR 121	1 2 1 1 1 1 1
2.		-8.2		
3.		-8.1		
4.		-8.0		
5.		-8.0		
6.		-7.8		
7.		-7.7		
8.		-7.6		
9.		-7.5		
10.		-7.4		

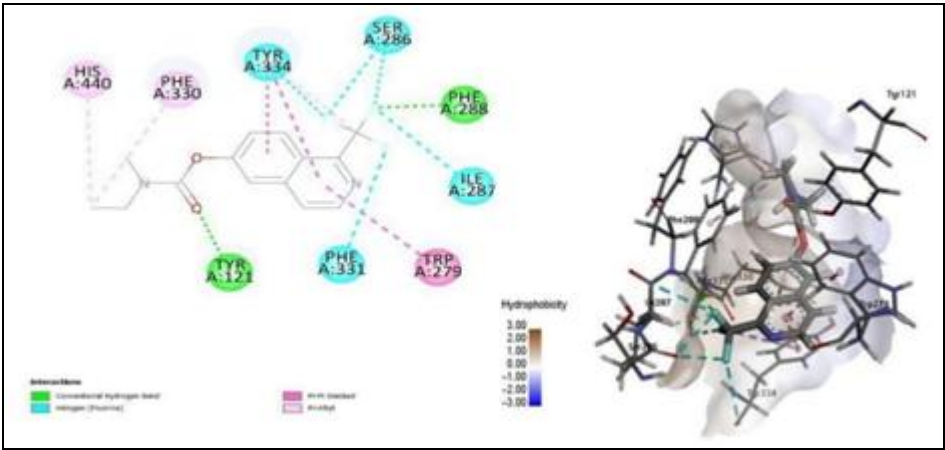


FIG. 25: 2D AND 3D INTERACTION DIAGRAM OF SELECTED 1FSS ISO-10 DOCK COMPLEX

After interaction analysis, screening, and ranking of the ligand poses in dock result, the complex with a binding affinity of -8.0 kcal/mol formed two hydrogen bonds with PHE 288 and TYR 121 were subjected to Molecular dynamic simulation.

TABLE 9: H-BOND ANALYSIS AFTER MD SIMULATION

Sl. no.	Protein	Ligand Name	H-Bond Interactions	MD
1.	1FSS	ISO-10	PHE 288, TYR 121	No H-bond Interaction

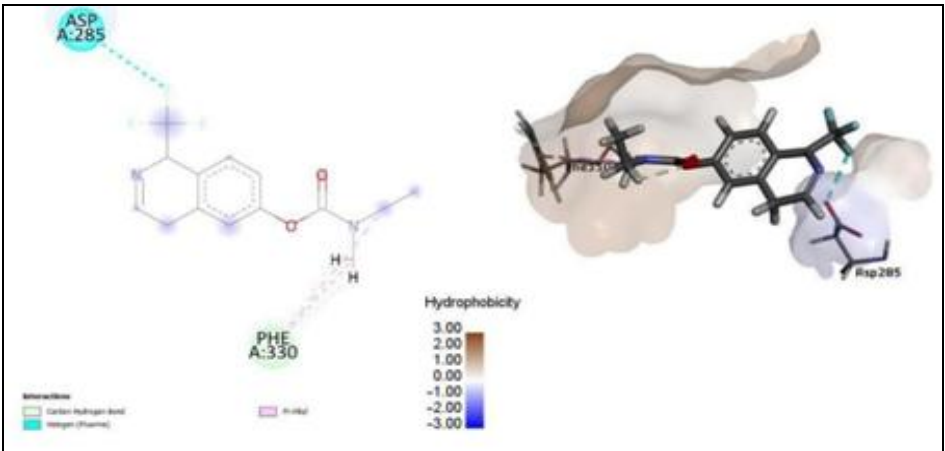


FIG. 26: 2D AND 3D INTERACTION DIAGRAM OF 1FSS – ISO-10 MD SIMULATED COMPLEX

RMSD, RMSF, Radius of gyration, Number of hydrogen bonds, and SASA plots were retrieved from the trajectory files to estimate the stability of the complex. The trajectory plots of the 1FSS ISO-10 complex are given below.

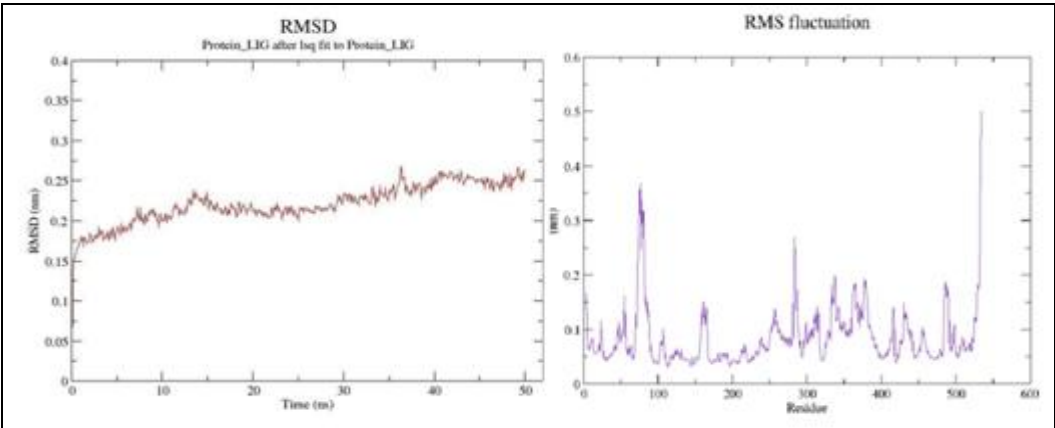


FIG. 27: RMSD AND RMSF PLOTS OF 1FSS ISO-10 MD SIMULATED COMPLEX

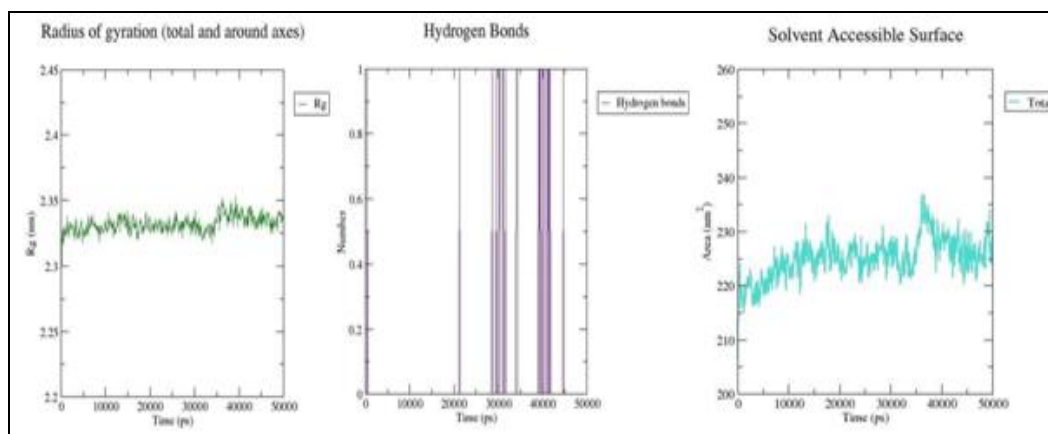


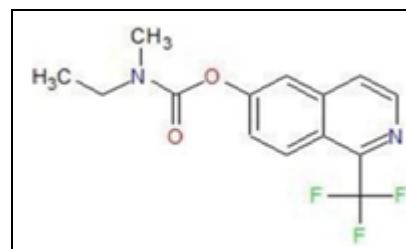
FIG. 28: RADIUS OF GYRATION PLOT, HYDROGEN BOND OCCUPANCY PLOT AND SASA PLOT

The RMSD values of the plot vary from a minimum of 0.1340096 nm at 0.1 ns to a maximum of 0.2682072 nm at 36.3 ns. This plot implies the protein does not undergo significant structural changes over the simulation time frame. The RMSF plot of the 1FSS ISO-10 complex shows that the entire protein shows fluctuation between 0.0308 nm and 0.5009 nm. Among these, THR 535 (0.5009 nm) has the highest fluctuation. The RoG plot of 1FSS ISO-10 complex inferred that the Rg deviation ranges from 2.31419 nm (0.2ns) to 2.3527 nm (39.3 ns), with an average of 2.331932 nm. The SASA plot of the 1FSS ISO-10 complex implies that fluctuations of the entire structure range between 214.997 nm² (1.2 ns) to 236.744 nm² (36.2 ns). The SASA value at 0th ns is 206.492 nm² and at 50th ns is 228.919 nm². Thus, the compound ISO-10 was accessed to be unstable in the molecular simulation study and thus assumes to be modified structurally for future development.

CONCLUSION: This research work was focused on the rational approach to design and develop Novel Carbamate- Heterocyclic conjugates with the aim of identifying potential drug targets for the management of Alzheimer's Disease. In *in-silico* modeling, it is found that the designed conjugates possess Anti- Alzheimer's activity with multi target activation.

The compound ISO-10 showed high binding affinity with the three targets AChE, NMDA, and Tyrosinase but the simulation studies showed that for 50 ns there were no stable hydrogen bonds. Thus, we assume that the compound ISO-10 may be structurally modified by the addition of more electronegative groups, hydrogen bond donors or hydrogen bond acceptors, heteroatoms (like

Oxygen, Nitrogen, Sulphur) for better hydrogen bonding, or by introducing additional ionic interactions which can enhance overall stability through salt bridges making it as a potential candidate for Anti Alzheimer's drug discovery.



ISO-10 [1-(TRIFLUOROMETHYL) ISOQUINOLIN-6-YL ETHYL (METHYL) CARBAMATE]

ACKNOWLEDGEMENT: The authors are thankful to the College of Pharmaceutical Sciences, Govt. Medical College, Thiruvananthapuram and Accubits Invent Private Limited, Bio 360 Life Sciences Park, Thiruvananthapuram for providing all the facilities regarding the work.

CONFLICTS OF INTEREST: Nil

REFERENCES:

1. Breijyeh Z and Karaman R: Comprehensive Review on Alzheimer's Disease: Causes and Treatment. *Molecules* 2020; 25: 5789.
2. Kamatham PT, Shukla R, Khatri DK and Vora LK: Pathogenesis, diagnostics, and therapeutics for Alzheimer's disease: Breaking the memory barrier. *Ageing Res Rev* 2024; 101: 102481.
3. Zhang XX, Tian Y, Wang ZT, Ma YH, Tan L and Yu JT: The Epidemiology of Alzheimer's Disease Modifiable Risk Factors and Prevention. *Journal of Prevention of Alzheimer's Disease* 2021; 8: 313–21. Available from: <https://link.springer.com/article/10.14283/jpad.2021.15>
4. Kumar A, Sidhu J, Lui F and Tsao JW: Alzheimer Disease [Internet]. *StatPearls*. StatPearls Publishing; 2024; 1–27. Available from: <https://www.ncbi.nlm.nih.gov/books/NBK499922/>

5. van Oostveen WM and de Lange ECM: Imaging techniques in alzheimer's disease: a review of applications in early diagnosis and longitudinal monitoring. *International Journal of Molecular Sciences* 2021; 22: 2110. Available from: <https://www.mdpi.com/1422-0067/22/4/2110/htm>
6. Zhang J, Zhang Y, Wang J, Xia Y, Zhang J and Chen L: Recent advances in Alzheimer's disease: mechanisms, clinical trials and new drug development strategies. *Signal Transduction and Targeted Therapy* 2024; 9: 1–35. Available from: <https://www.nature.com/articles/s41392-024-01911-3>
7. Cheong SL, Tiew JK, Fong YH, Leong HW, Chan YM and Chan ZL: Current Pharmacotherapy and Multi-Target Approaches for Alzheimer's Disease. *Pharmaceuticals* 2022; 15: 1560. Available from: <https://www.mdpi.com/1424-8247/15/12/1560/htm>
8. Matošević A and Bosak A: Carbamate group as structural motif in drugs: a review of carbamate derivatives used as therapeutic agents. *Archives of Industrial Hygiene and Toxicology* 2020; 71: 285. Available from: <https://pmc.ncbi.nlm.nih.gov/articles/PMC7968508/>
9. Ozten O, Zengin Kurt B, Sonmez F, Dogan B and Durdagi S: Synthesis, molecular docking and molecular dynamics studies of novel tacrine-carbamate derivatives as potent cholinesterase inhibitors. *Bioorg Chem* 2021; 115: 105225.
10. Wang F, Yao Y, Zhu H liang and Zhang Y: Nitrogen-containing Heterocycle: A Privileged Scaffold for Marketed Drugs. *Curr Top Med Chem* 2021; 21: 439–41.
11. Obaid RJ, Naeem N, Mughal EU, Al-Rooqi MM, Sadiq A and Jassas RS: Inhibitory potential of nitrogen, oxygen and sulfur containing heterocyclic scaffolds against acetylcholinesterase and butyrylcholinesterase. *RSC Adv* 2022; 12: 19764–855. Available from: <https://pubs.rsc.org/en/content/articlehtml/2022/ra/d2ra03081k>
12. Zeng W, Han C, Mohammed S, Li S, Song Y and Sun F: Indole-containing pharmaceuticals: targets, pharmacological activities, and SAR studies. *RSC Med Chem* 2024; 15: 788–808. Available from: <https://pubs.rsc.org/en/content/articlehtml/2024/md/d3md00677h>
13. Jasiewicz B, Kozanecka-Okupnik W, Przygodzki M, Warżajtis B, Rychlewska U and Pospieszny T: Synthesis, antioxidant and cytoprotective activity evaluation of C-3 substituted indole derivatives. *Scientific Reports* 2021; 11: 1–14. Available from: <https://www.nature.com/articles/s41598-021-94904-z>
14. Shah M, Parmar R, Patel K and Nagani A: Indole-based COX-2 inhibitors: A decade of advances in inflammation, cancer, and Alzheimer's therapy. *Bioorg Chem* 2024; 153.
15. Mo X, Rao DP, Kaur K, Hassan R, Abdel-Samea AS and Farhan SM: Indole derivatives: a versatile scaffold in modern drug discovery an updated review on their multifaceted therapeutic applications. *Molecules* 2024; 29: 4770. Available from: <https://www.mdpi.com/1420-3049/29/19/4770/htm>
16. Danao KR, Malghade PM, Mahapatra DK, Motiwala MN and Mahajan UN: Progressive insights into the pharmacological importance of isoquinoline derivatives in modern therapeutics. *Int J Curr Res Rev* 2021; 13: 83–90.
17. Paithankar VR, Dighe PR and Shinde NV: An Overview of Thiazole Derivatives and its Biological Activities. *Int J Pharm Sci Rev Res* 2023; 42–7.
18. Joshi S, Mehra M, Singh R and Kakar S: Review on Chemistry of Oxazole derivatives: Current to Future Therapeutic Prospective. *Egyptian Journal of Basic and Applied Sciences* 2023; 10: 218–39. Available from: <https://www.tandfonline.com/doi/abs/10.1080/2314808X.2023.2171578>
19. Kushwaha N and Sharma CS: The Chemistry of Triazine Isomers: Structures, Reactions, Synthesis and Applications. *Mini Rev Med Chem* [Internet]. 2020 [cited 2025; 20: 2104–22. Available from: <https://pubmed.ncbi.nlm.nih.gov/32727324/>
20. Pal R, Kumar B, Swamy PMG and Chawla PA: Design, synthesis of 1,2,4-triazine derivatives as antidepressant and antioxidant agents: *In-vitro*, *in-vivo* and *in-silico* studies. *Bioorg Chem* 2023; 131: 106284.
21. RCSB PDB - 1FSS: Acetylcholinesterase (E.C. 3.1.1.7) complexed with Fasciculin-II [Internet]. [cited 2025 Feb 10]. Available from: <https://www.rcsb.org/structure/1FSS>
22. Dileep KV, Ihara K, Mishima-Tsumagari C, Kukimoto-Niino M, Yonemochi M and Hanada K: Crystal structure of human acetylcholinesterase in complex with tacrine: Implications for drug discovery. *Int J Biol Macromol* 2022; 210: 172–81.
23. Chou TH, Epstein M, Michalski K, Fine E, Biggin PC and Furukawa H: Structural insights into binding of therapeutic channel blockers in NMDA receptors. *Nature Structural & Molecular Biology* 2022 29:6 [Internet]. 2022 [cited 2025 Jan 31]; 29: 507–18. Available from: <https://www.nature.com/articles/s41594-022-00772-0>
24. Siddiqui AJ, Badraoui R, Jahan S, Alshahrani MM, Siddiqui MA and Khan A: Targeting NMDA receptor in Alzheimer's disease: identifying novel inhibitors using computational approaches. *Front Pharmacol* [Internet]. 2023 [cited 2025 Jan 31]; 14: 1208968. Available from: <https://plasma-gate.weizmann.ac.il/Grace/>.
25. RCSB PDB - 7SAD: Memantine-bound GluN1a-GluN2B NMDA receptors [Internet]. [cited 2025 Feb 1]. Available from: <https://www.rcsb.org/structure/7SAD>
26. Ge Z, Liu JC, Sun JA and Mao XZ: Tyrosinase inhibitory peptides from enzyme hydrolyzed royal jelly: production, separation, identification and docking analysis. *Foods* [Internet]. 2023 [cited 2025 Jan 31]; 12: 2240. Available from: <https://pmc.ncbi.nlm.nih.gov/articles/PMC10252203/>
27. Gautam D, Naik UP, Naik MU, Yadav SK, Chaurasia RN and Dash D: Glutamate receptor dysregulation and platelet glutamate dynamics in alzheimer's and parkinson's diseases: insights into current medications. *Biomolecules* 2023; 1609 [Internet]. 2023 [cited 2025 Mar 26]; 13: 1609. Available from: <https://www.mdpi.com/2218-273X/13/11/1609/htm>
28. Ladagu AD, Olopade FE, Adejare A and Olopade JO: GluN2A and glun2b n-methyl-d-aspartate receptor (nmdars) subunits: their roles and therapeutic antagonists in neurological diseases. *Pharmaceuticals* [Internet]. 2023 [cited 2025 Feb 6]; 16: 1535. Available from: <https://pmc.ncbi.nlm.nih.gov/articles/PMC10674917/>
29. Li J, Feng L, Liu L, Wang F, Ouyang L and Zhang L: Recent advances in the design and discovery of synthetic tyrosinase inhibitors. *Eur J Med Chem* 2021; 224: 113744.
30. RCSB PDB - 5I38: Crystal Structure of tyrosinase from *Bacillus megaterium* with inhibitor kojic acid in the active site [Internet]. [cited 2025 Jan 31]. Available from: <https://www.rcsb.org/structure/5I38>
31. Ivanović V, Rančić M, Arsić B and Pavlović A: Lipinski's rule of five, famous extensions and famous exceptions. *Chemia Naissensis* [Internet]. 2020 [cited 2025 Mar 28]; 3: 171–81. Available from: https://www.researchgate.net/publication/371277639_Lipi

- nski's_rule_of_five_famous_extensions_and_famous_exceptions
32. Way2Drug - main [Internet]. [cited 2025 Feb 1]. Available from: <https://www.way2drug.com/passonline/>
 33. Sharma I, Khurana N, Muduli SK and Sharma N: Systematic Review and PASS Assisted Prediction of Selected Phytoconstituents for Alzheimer's Disease. AIP Conf Proc [Internet]. 2023 [cited 2025 Mar 27]; 2800. Available from: </aip/acp/article/2800/1/020192/2910174/Systematic-review-and-PASS-assisted-prediction-of>
 34. SwissADME [Internet]. [cited 2025 Feb 1]. Available from: <http://www.swissadme.ch/>
 35. Subramanian A, Tamilanban T, Subramaniyan V, Sekar M, Kumar V and Janakiraman AK: Establishing network pharmacology between natural polyphenols and Alzheimer's disease using bioinformatic tools – An advancement in Alzheimer's research. Toxicol Rep 2024; 13: 101715.
 36. Şahin S and Dege N: A newly synthesized small molecule: the evaluation against Alzheimer's Disease by *in-silico* drug design and computational structure analysis methods. J Mol Struct 2021; 1236: 130337.
 37. Ji D, Ma J, Dai J, Xu M, Harris PWR and Brimble MA: Anticholinesterase inhibition, drug-likeness assessment, and molecular docking evaluation of milk protein-derived opioid peptides for the control of alzheimer's disease. Dairy 2022; Vol 3, Pages 422-437 [Internet]. 2022 [cited 2025 Feb 10]; 3: 422–37. Available from: <https://www.mdpi.com/2624-862X/3/3/32/htm>
 38. Ali BL and Shabeer TK: Identifying clinically significant novel drug candidate for highly prevalent Alzheimer's disease. Indian Journal of Chemical Technology [Internet]. 2021 [cited 2025 Mar 27]; 28: 618–23. Available from: <http://www.pdb.org>
 39. SwissTargetPrediction [Internet]. [cited 2025 Feb 22]. Available from: <http://www.swisstargetprediction.ch/about.php>
 40. Şahin S. A single-molecule with multiple investigations: Synthesis, characterization, computational methods, inhibitory activity against Alzheimer's disease, toxicity, and ADME studies. Comput Biol Med 2022; 146: 105514.

How to cite this article:

Hameed SA, Fathima N, Gadha S, Gopika MS, Namitha RV and Sahadiya: Molecular mavericks: exploring carbamate-heterocycle conjugates in the quest for effective alzheimer's therapy. Int J Pharm Sci & Res 2025; 16(8): 2275-93. doi: 10.13040/IJPSR.0975-8232.16(8).2275-93.

All © 2025 are reserved by International Journal of Pharmaceutical Sciences and Research. This Journal licensed under a Creative Commons Attribution-NonCommercial-ShareAlike 3.0 Unported License.

This article can be downloaded to **Android OS** based mobile. Scan QR Code using Code/Bar Scanner from your mobile. (Scanners are available on Google Playstore)